Optical Fiber Surface Plasmon Resonance for Glucose Detection

Cristina Cunha[1,2], *Susana* Silva[1], *Luís C. C.* Coelho[1], *Orlando* Frazão[1] and *Susana* Novais[1,*]

[1] INESC TEC – Institute for Systems and Computer Engineering, Technology and Science, Porto, Portugal
[2] Department of Physics and Astronomy, Faculty of Sciences of University of Porto

Abstract. This work proposes a sensor that utilizes a transmission scheme for measuring glucose aqueous solutions based on surface plasmon resonance. A comparison between the performance of two sensors with similar lengths and different diameters is performed. The first sensor comprises a multimode optical fiber with a diameter of 400 μm and a 10 *mm* middle section of the cladding removed. The second sensor is similar, except that the fiber has a diameter of 600 μm. The sensors were evaluated for their performance in measuring glucose concentrations ranging from 0.0001 to 0.5000 *g/mL*. The 400 μm sensor demonstrated high sensitivity however, the sensor with a diameter of 600 µm attained a slightly higher maximum sensitivity of 322.0 *nm/(g/mL)*.

1 Introduction

The most widely distributed and significant monosaccharide in nature is glucose. It is crucial to human life, health, and the biomedical field. Therefore, the importance of glucose detection and its potential commercial value has continuously driven research efforts in the scientific community to explore various methods for developing glucose sensors, such as electrochemical sensing [1], optical fiber sensors (OFS) [2], and chemiluminescence techniques [3]. Using surface resonance (SPR) as a sensitivity enhancer, this work describes the development of a transmissive multimode optical fiber gold (Au) that measures glucose concentration.

2 Sensor and Operation Principle

The sensing device consists of a large diameter step-index multimode fiber functionalized with Au coating. Two distinct silica fibers were used, with core diameters of 400 and 600 μm, respectively, (FT400ETM and FT600EMT, Thorlabs, USA), with a max attenuation of 10 *dB/km* at 800 *nm*). To produce each sensor, a 150 *mm* segment of optical fiber was sliced, with 30 *mm* being removed from each end with a blade. To remove the remaining coating, a cloth was soaked in ethanol and applied to the stripped area. An optical microscope inspection was also done to ensure the cladding was taken off. The coating in the middle section of the fiber with 10 *mm* was removed leaving an uncoated detection region. Afterward, a 50 *nm* Au nanocoating was deposited on the 10 *mm* long uncoated middle section of each multimode optical fiber, using a sputter coater (Leica EM SCD500), which operated with an Au target bombarded with argon ions. In Figure 1 it is possible to observe the schematic diagram of the sensor structure.

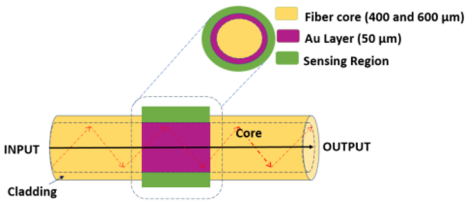

Fig. 1. Optical fiber sensor configuration.

Parallel to the Au target, optical fiber batches of 400 and 600 μm were positioned inside the chamber. As a result, a 180º rotation was required to ensure that the fibers sensing the region's surface were completely coated. Due to having a greater sensor area to cover, the 600 μm fibers had an exposure time of 120 seconds whereas the 400 μm fibers were subjected to 80 seconds of Au deposition.
Lastly, to improve the Au film's adherence to the silica surface the Au sensors were annealed in a heat chamber for two hours at 180 °C. Figure 2 presents the scheme of the experimental setup used in this work. The sensing structure spectral response was observed in a transmission scheme and it is composed of a halogen lamp (Tungsten-Halogen Light Source, manufactured by Sarspec, Portugal) and a spectrometer (from Ocean Optics). Firstly, the white light source (that has an emission range from 600 to 1100 *nm*) is connected to SMA patch cables, and the sensing probe, being the last one linked to a spectrometer connected to a laptop.

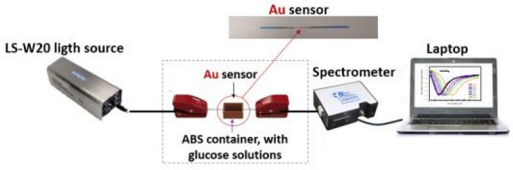

Fig. 2. Scheme of the experimental setup.

The spectra were monitored in real-time using the software Spectra Suite, from Ocean Optics, and the data

* Corresponding author: susana.novais@inestec.pt

© The Authors, published by EDP Sciences. This is an open access article distributed under the terms of the Creative Commons Attribution License 4.0 (https://creativecommons.org/licenses/by/4.0/).

acquired was processed in the software Origin 2018 64 Bit.

2.1. Results and Discussion

SPR is a phenomenon that happens when the evanescent wave's vector coincides with the surface plasmons wave vector. The sensor can identify variations in refractive index (RI) since the wave vector depends on the medium's RI. The sensor can identify the concentrations of glucose solutions since different concentrations are proportional linearly to the respective RI. The samples were measured using an Abbe refractometer (ATAGO, DR-A1) to estimate the RI of glucose solutions. The samples got optically denser as the solution's glucose concentration rises, causing a linear increase in RI (Figure 2).

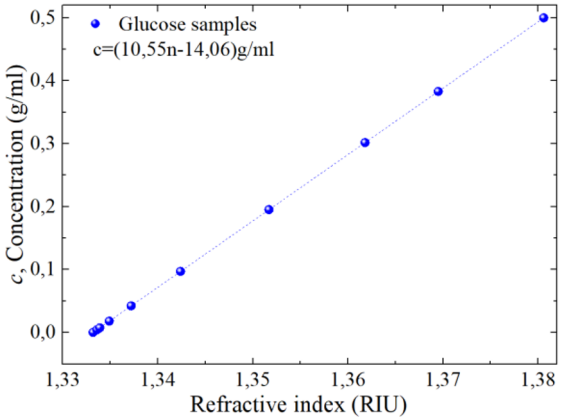

Fig. 2. Concentration of glucose in solution as a function of refractive index.

A collective oscillation of the electrons known as a surface plasmon is produced when a broad-spectrum light source excites the conduction electrons in the Au layer. When the surface plasmon is activated, an evanescent field is also generated in the unclad area of the fiber. This field penetrates the medium and decays exponentially, making it sensitive to variations in the medium's RI and consequently to concentration variations. In the inset of Figure 3, it is shown the shifts in the normalized transmission spectra from direct exposure of the Au sensors under different concentrations of glucose. Based on the analysis of the obtained spectra, it can be concluded that the position of the SPR signatures undergoes a red shift as the concentration values increase. The proposed sensor with a diameter of 400 μm demonstrated high sensitivity, with a total wavelength redshift of 117.3 *nm*, whereas the sensor with a diameter of 600 μm obtained a slightly higher wavelength redshift of 127.4 *nm*. The wavelength sensitivity was determined by derivate the resulting polynomial functions presented in Figure 3. Using this method, it is possible to collect accurate and punctual data for each concentration level, which helps establish a full understanding of the sensor's operation. The results of punctual sensitivities in each different glucose sample for both sensors are present in Table 1.

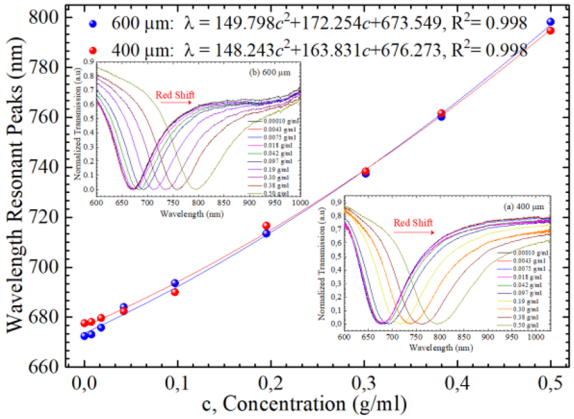

Fig. 3. Resonance peaks as a function of glucose concentration.

Table 1. Wavelength sensitivity of fiber sensors with different core diameters for detecting glucose concentrations.

Concentration (g/ml)	*Sensitivity nm/(g/ml) of the Au **600 µm** sensor*	*Sensitivity nm/(g/ml) of the Au **400 µm** sensor*
0.0010	172.283	163.861
0.0078	174.495	166.048
0.0180	177.655	169.176
0.0423	184.922	176.368
0.0971	201.352	192.627
0.1952	230.736	221.706
0.3017	262.647	253.286
0.3829	286.976	277.361
0.5000	322.048	312.069

The resolutions and stabilities of both sensors were also studied. The 400 μm sensor achieved a resolution of 0.027 *g/mL*, and the standard deviation for the stability study was 0.018 *nm/(g/mL)*. Meanwhile, the 600 μm sensor obtained a resolution of 0.028 *g/mL*, and the standard deviation was 0.022 *nm/(g/mL)*, indicating that both sensors have good stability.

Conclusion

Using a surface plasmon resonance-based transmission system, the comparison between two sensors for measuring glucose concentrations was suggested. The developed sensors showed similar stability and resolution. However, the 600 μm sensor demonstrated better wavelength sensitivity, and higher robustness makes it a better solution for monitoring and measuring glucose real-time concentration.

This work was financially supported by the Wellcome Trust, UK, through the Innovator Award "Light-activated cap for catheter sterilization" (WT223940/Z/21/Z). The work of S.Novais was supported by National Funds through the Portuguese funding agency, FCT-Fundação para a Ciência e a Tecnologia, within 2020.00044.CEECIND research contract.

References

1. W. Li, W. luo, M. Li, L. Chen, L. Chen, H. Guan, M. Yu, Front. Chem, **9** (2021)
2. P. Gong, X. Li, X. Zhou, Y. Zhang, N. Chen, S. Wang, S. Zhang, Y. Zhao, Opt Laser Technol , **139** (2021)
3. D. Yan, Y. Huang, S. Chen, W. Zuo, and B. Shi, Acs Omega **6** (2018)